Nanotechnology

DOI: 10.1002/anie.200604540

Evaporation-Induced Self-Assembly of Nanoparticles from a Sphere-on-Flat Geometry**

*Jun Xu, Jianfeng Xia, and Zhiqun Lin**

Self-assembly of nanoscale materials to form ordered structures promises new opportunities for developing miniaturized electronic, optoelectronic, and magnetic devices.[1–4] In this regard, several elegant methods based on self-assembly have emerged,[5–8] for example, self-directed self-assembly,[5] and electrostatic self-assembly.[8] Self-assembly of nanoparticles by irreversible solvent evaporation has been recognized as an extremely simple route to intriguing structures.[9–12] However, these dissipative structures are often randomly organized without controlled regularity. Herein, we show a simple, one-step technique to produce concentric rings and spokes comprising quantum dots or gold nanoparticles with high fidelity and regularity by allowing a drop of a nanoparticle solution to evaporate in a sphere-on-flat geometry. The rings and spokes are nanometers high, submicrons to a few microns wide, and millimeters long. This technique, which dispenses with the need for lithography and external fields, is fast, cheap and robust. As such, it represents a powerful strategy for creating highly structured, multifunctional materials and devices.

Quantum dots (QDs) are highly emissive, spherical, inorganic nanoparticles a few nanometers in diameter. They provide a functional platform for a new class of materials for use in light emitting diodes (LEDs),[13] photovoltaic cells,[14] and biosensors.[15] Because of the quantum-confined nature of QDs such as CdSe, the variation of particle size provides continuous and predictable changes in fluorescence emission. Passivating the vacancies and trap sites on the CdSe surface with higher-band-gap materials, such as ZnS, produces CdSe/ZnS core/shell QDs that have strong photoluminescence.[16] Two CdSe/ZnS core/shell QDs (4.4 and 5.5 nm in diameter, D) were used as the first nonvolatile solutes in our experiments. The surface of CdSe/ZnS was passivated with a monolayer of tri-n-octylphosphine oxide (TOPO) to impart solubility to the host environment and retain the spectroscopic properties of the materials by preventing them from aggregating. A drop of CdSe/ZnS in toluene was loaded in a confined geometry consisting of a spherical silica lens in contact with an Si substrate (i.e., sphere-on-flat geometry; see Experimental Section),[17–21] which led to the formation of a capillary bridge of the solution as illustrated in Figure 1a. In situ optical microscopy (OM) revealed two main types of pattern formations, namely, concentric rings and spokes, which depend on whether fingering instabilities of thin film of the evaporating front took place or not.

The formation of ringlike deposits in an evaporating drop that contains nonvolatile solutes on a single surface is known as the "coffee-ring" phenomenon.[9,10,22,23] Maximum evaporative loss of the solvent at the perimeter triggers the jamming of the solutes and creates a local roughness (i.e., the contact

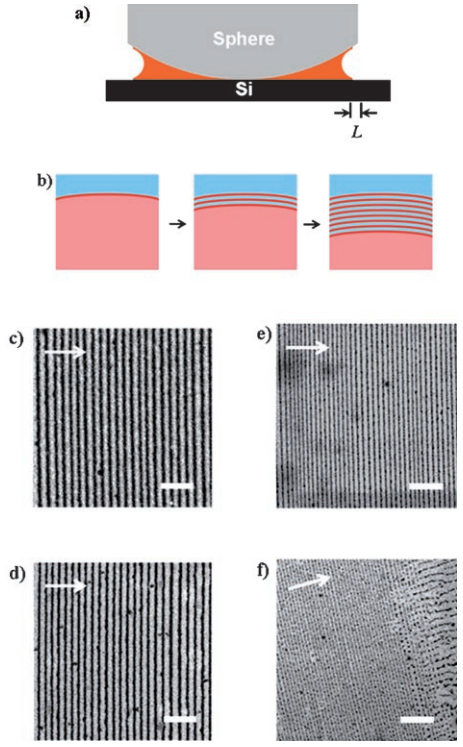

Figure 1. a) Sphere-on-flat geometry in which a drop of nanoparticle solution is constrained, thus bridging the gap between the spherical lens and Si substrate. b) Stepwise representation of the formation of concentric rings, which propagate from the capillary edge of the drop towards the center of the sphere/Si contact. c–f) SEM images of concentric rings produced by evaporation-induced self-assembly of 5.5-nm CdSe/ZnS QDs formed by drying 0.25 mg mL^{-1} (c), 0.15 mg mL^{-1} (d), and 0.05 mg mL^{-1} (e and f) toluene solutions. A transition from rings to wirelike structures (c = 0.05 mg mL^{-1}) is shown on the right side of panel (f). The scale bar is 20 μm in (c–e) and 30 μm in (f). The white arrow on the upper left marks the direction of the movement of the solution front.

[*] J. Xu, J. Xia, Prof. Z. Lin
Department of Materials Science and Engineering
Iowa State University
Ames, IA 50011 (USA)
Fax: (+1) 515-294-7202
E-mail: zqlin@iastate.edu
Homepage: http://www.mse.iastate.edu/zqlin

[**] This work was supported by the DOE Ames Lab seed funding, the 3M Nontenured Faculty Award, and the NSF-NIRT-0506832. J.X. thanks the Institute for Physical Research and Technology of Iowa State University for a Catron graduate research fellowship.

Supporting information for this article is available on the WWW under http://www.angewandte.org or from the author.

line is pinned). This action leads to the transportation of solutes to the edge, thus forming a coffee-ring stain.[9,10,22,23] The repeated "stick–slip" motions of the contact line produce concentric rings governed by the competition between the capillary force and the pinning force.[18] However, stochastic rings (irregular multirings) are generally formed on a single surface.[22,23] In contrast, highly ordered concentric rings composed of 5.5 nm CdSe/ZnS QDs over a distance of hundreds of micrometers were created by drying a toluene solution of QDs ($c = 0.25\ \mathrm{mg\,mL^{-1}}$) in a sphere-on-flat geometry (Figure 1 b,c). This pattern is a direct consequence of the controlled, repetitive pinning and depinning cycles of the contact line (Figure 1 b), which resembles our recent findings on the self-assembly of polymeric materials.[17,18,24] According to in situ OM observation, it took about 7 s for a ring to deposit (stick); a 0.5 s "slip" followed. Thus, the solution front speed was estimated to be: $v = 9\ \mu\mathrm{m\,s^{-1}}$ (slip over a distance of 4.7 μm in 0.5 s). Locally, the concentric rings appeared as parallel stripes. The center-to-center distance between the adjacent rings, $\lambda_{c\text{-}c}$, and the width of the ring, w, were 4.7 μm and 2.2 μm, respectively, as determined by fast Fourier transformation of AFM and SEM images. The average height of the rings measured by AFM was 13.2 nm. The observations of QD rings with remarkable regularity highlight the significance of using a sphere-on-Si geometry, which is extremely easy to implement, to guide solvent evaporation and control capillary flow in a drying drop.

Figures 1 d and e show that an array of periodic rings of QDs was also obtained at lower solution concentrations ($c = 0.15\ \mathrm{mg\,mL^{-1}}$ in Figure 1 d and $0.05\ \mathrm{mg\,mL^{-1}}$ in Figure 1 e). The ring patterns in Figures 1 c–e reveal a noteworthy influence of the concentration on the resulting dimension of the QDs. For the 5.5 nm QD toluene solution, the ring width, w, decreased from 2.2 μm at $c = 0.25\ \mathrm{mg\,mL^{-1}}$ (Figure 1 c) to 1.5 μm at $c = 0.15\ \mathrm{mg\,mL^{-1}}$ (Figure 1 d), and to 630 nm at $c = 0.05\ \mathrm{mg\,mL^{-1}}$ (Figure 1 e). It should be noted that these submicron-wide rings (630 nm) were, for the first time, obtained by solvent evaporation in a sphere-on-flat geometry.[17,18] A similar trend was seen in $\lambda_{c\text{-}c}$, which decreased from 4.7 μm at $c = 0.25\ \mathrm{mg\,mL^{-1}}$ to 4.0 μm at $c = 0.15\ \mathrm{mg\,mL^{-1}}$, and to 2.9 μm at $c = 0.05\ \mathrm{mg\,mL^{-1}}$ (Figure 1 c–e). The average height of rings, h, was 6.9 nm and 5.5 nm at $c = 0.15$ and $0.05\ \mathrm{mg\,mL^{-1}}$, respectively. A larger value of h implies a longer pinning time of QDs at the three-phase contact line, which, in turn, causes a larger w and a greater evaporation volume loss of toluene during pinning.[18] As a result, there is a larger pull on the contact line to a new position. Thus, a larger $\lambda_{c\text{-}c}$ was observed at a higher concentration of the solution.[18,23,25] It is noteworthy that constant values of $\lambda_{c\text{-}c}$ and w were observed at a given concentration. This consistency can be attributed to the uniform h of QDs deposited on the substrates, which suggests a constant pinning time. Thus, the evaporative loss of solvent was steady and led to the formation of concentric rings with constant $\lambda_{c\text{-}c}$ and w.

Note that at a late stage of drying, all three 5.5-nm CdSe/ZnS QD toluene solutions ($c = 0.25$, 0.15, and $0.05\ \mathrm{mg\,mL^{-1}}$) in which the solution front was very close to the center of the sphere/Si contact, exhibited a transition from concentric rings to radially aligned wirelike patterns (see top right in Figure 1 f). This change can be rationalized as follows: the velocity of the displacement of the meniscus, v (i.e., the solution front in Figure 1 a), in a capillary bridge is inversely proportional to the distance from the capillary entrance to the meniscus, L (i.e., $v \approx 1/L$);[26] v decreases as the meniscus moves inward as a result of an increase in L (Figure 1 a). It has been numerically demonstrated that the formation of fingering instability in an evaporating film is dictated by v: a faster v stabilizes the front, whereas a slower v leads to the development of fingering instabilities at a propagating front.[27] In this study, as the solution front retracted, the evaporation rate of the solvent decreased, which caused a reduction in v. As a consequence, the concentration and the viscosity of the solution at the meniscus decreased, which led to instabilities.[27]

A fluorescence microscopic image of concentric rings obtained from self-assembling 5.5-nm CdSe/ZnS QDs after toluene evaporation ($c = 0.15\ \mathrm{mg\,mL^{-1}}$) is shown in Figure 2

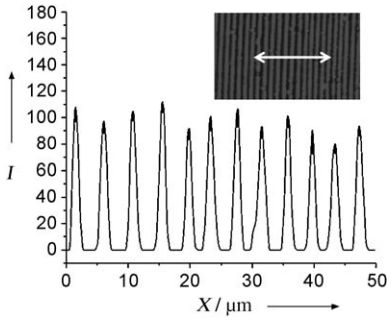

Figure 2. Scan of fluorescence intensity along the arrow indicated in the fluorescence microscopic image (inset, converted into gray scale) of CdSe/ZnS rings. The rings were produced by self-assembly of 5.5-nm CdSe/ZnS QDs after toluene evaporation from a $0.15\ \mathrm{mg\,mL^{-1}}$ solution.

as an inset. The fluorescence intensity (Figure 2) oscillates almost evenly over a 50 μm scanning distance (arrow in the inset), thus signifying that the rings have uniform height and width. A periodic spacing between rings is also clearly evident. The ability to deposit fluorescent nanoparticles with well-defined dimensions in the concentric-ring mode presented herein may open a very simple route to manipulating linear micron-to-submicron wires of semiconductors into a ring structure for use in ring resonator lasers.[28]

It should be noted that a film with chaotic structures was observed from a control sample in which the QD toluene solution ($V = 12\ \mu\mathrm{L}$, $c = 0.25\ \mathrm{mg\,mL^{-1}}$, $D = 5.5$ nm) was allowed to evaporate on a silicon substrate with or without a cover for preventing possible convections (see Supporting Information). This observation justified the necessity of employing the sphere-on-flat configuration to control the evaporation process and associated capillary flow. In a second control experiment, an extra amount of coordinating ligand, TOPO, was added to the QD solutions. Irregular, discontinuing patterns were seen (see Supporting Information). Therefore, to obtain well-ordered rings, the excessive TOPO was

removed to leave only TOPO-covered nanoparticles that were used in the experiments.

Instead of concentric rings as seen parallel to the three-phase contact line at the early stage of the solvent evaporation when the 5.5-nm CdSe/ZnS QDs were used (Figures 1 and 2), spokes were produced exclusively throughout the entire drying process when a smaller CdSe/ZnS QD ($D = 4.4$ nm) was used. The speed of the solution front, which moved in a continuous manner, was $v = 1\ \mu m\,s^{-1}$ during the formation of spokes, as evaluated by in situ OM observation. The dynamic formation of spokes is attributed to the fingering instabilities of the evaporating front,[6,7,27,29–31] as illustrated in Figure 3a. At an early stage of the drying process, the fingers form at the

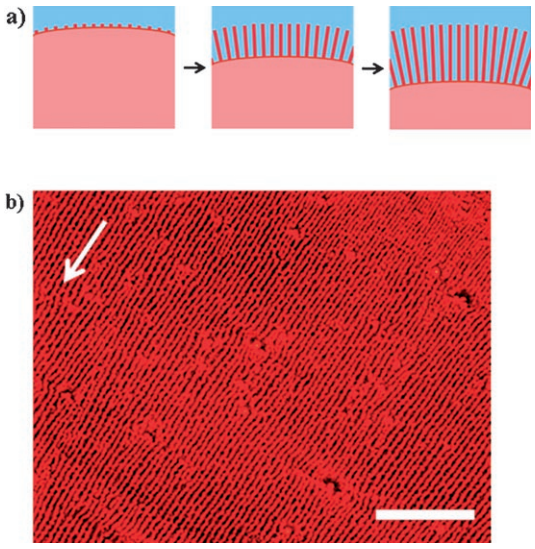

Figure 3. a) Formation of spoke patterns upon evaporation from the capillary bridge in the sphere-on-flat geometry. b) Optical micrograph showing the spokes formed by drying 4.4-nm CdSe/ZnS toluene solution ($c = 0.25\ mg\,mL^{-1}$). The scale bar is 100 μm. The arrow on the upper left indicates the direction of the movement of the solution front.

three-phase contact line (first panel in Figure 3a). They serve as nucleation sites and grow into stripes locally that orient normal to the evaporating front by transporting the QDs from the surrounding solution (second panel in Figure 3a) as they propagate inward. This process results in spoke patterns (last panel in Figure 3a).[7] The process is analogous to the molecular combing of DNA chains, in which DNA chains are aligned perpendicular to the contact line of a drying drop.[32] Figure 3b shows a typical fluorescence microscopic image of a dried film comprising 4.4-nm CdSe/ZnS QDs. Each stripe in the spoke was 22 nm high, 1.8 μm wide, and millimeters long. The distance between adjacent stripes, λ_f, was 5 μm. The movement of the solution front with 4.4-nm QDs ($v = 1\ \mu m\,s^{-1}$) was much slower than that with 5.5-nm QDs ($v = 9\ \mu m\,s^{-1}$ per slip) at the same concentration ($c = 0.25\ mg\,mL^{-1}$). The smaller v facilitated the formation of fingering instability at the solution front.[27] Thus, spokes were formed with 4.4-nm QDs, while rings were produced with 5.5-nm QDs.

To further demonstrate that a wide variety of nanoparticles can be used to produce regular patterns in the sphere-on-flat geometry, CdTe nanorods (7 nm in diameter and 20 nm in length) and Au nanoparticles (6 nm in diameter) were also employed (see Experimental Section). Concentric ring patterns consisting of CdTe nanorods and Au nanoparticles (see Supporting Information) were observed. We note that the CdTe nanorods and Au nanoparticles were larger than the CdSe/ZnS QDs. Larger surface roughness and a stronger pinning force are expected with larger nanoparticles. Therefore, rather than spokes, the concentric rings dominate exclusively in CdTe and Au nanoparticles despite the fact that the nanoparticles used in our studies (CdSe/ZnS, CdTe, and Au) were all passivated with the same ligand, TOPO.

In summary, we have demonstrated that constrained evaporation (i.e., drying in a confined, axial symmetric geometry to provide control over the solvent evaporation and the associated capillary flow) can be utilized as a simple, cheap, and robust strategy for self-assembling various nanoparticles with easily tailored optical and electronic properties into spatially ordered, two-dimensional patterns of a single layer or several layers of particle thickness on the micrometer-to-submicron scale. These self-organized patterns of functional nanoscale materials over large areas offer a tremendous potential for applications in optoelectronic devices, LEDs, solar cells, and biosensors.

Experimental Section

Materials: Two kinds of TOPO-functionalized CdSe/ZnS core/shell QDs[16] were prepared in accordance with previous reports.[33] The diameters of the QDs were 4.4 and 5.5 nm as determined by TEM, which correspond to the growth of two-to-three atomic layers of ZnS, provided that the original CdSe are 3.0 and 4.0 nm in diameter. The 4.4-nm QDs were orange-emitting with the maximum emission, λ_{max}, at 598 nm. The 5.5-nm QDs were red-emitting with λ_{max} at 632 nm. The QDs were purified twice by using antisolvent precipitation from the reaction mixture in chloroform, thus removing excessive TOPO ligand. They were subsequently vacuum-dried and dissolved in toluene to make a stock solution ($1\ mg\,mL^{-1}$). Finally, QD toluene solutions at different concentrations (0.25, 0.15, and 0.05 $mg\,mL^{-1}$ for the 5.5-nm QDs) were prepared by diluting the filtered stock solution (syringe filter with 200 nm pore size). TOPO-covered CdTe short nanorods (7 nm in diameter and 20 nm in length; Supporting Information) and TOPO-covered Au nanoparticles (6 nm in diameter) were also synthesized and purified in accordance with previous reports.[33,34]

Pattern formation in the sphere-on-flat geometry: A drop of a solution of nanoparticles in toluene (12 μL; CdSe/ZnS QDs, CdTe nanorods or Au nanoparticles) was loaded in a small gap between a spherical silica lens and a SiO_2-coated Si wafer (thermally coated 300 nm thick SiO_2 on Si). The sphere and Si wafer were firmly fixed at the top and bottom, respectively, of a sample holder inside a sealed chamber. The temperature inside the chamber was rigorously monitored and was constant during the experiment. The two surfaces (sphere and Si wafer) were brought into contact, thus forming a capillary bridge of the solution.[17,18] The diameter and radius of curvature of the sphere were 1 cm and 2 cm, respectively. In such sphere-on-flat geometry, evaporation occurred only at the capillary edge. It took approximately 30 min for the evaporation to be complete. Finally, the two surfaces were separated and the patterns on the Si wafer were examined.

Characterization: In situ optical microscopy (Olympus BX51) was performed in reflective mode under bright light. AFM imaging of patterns on an Si surface was obtained by using a scanning force microscope (Digital Instruments Dimension 3100) in tapping mode. SEM studies were performed on a Hitachi S-4000 field-emission scanning electron microscope operating at 10 kV accelerating voltage. TEM studies were performed on a JEOL 1200EX scanning/transmission electron microscope operating at 80 kV.

Received: November 6, 2006
Published online: January 24, 2007

Keywords: molecular devices · nanotechnology · quantum dots · self-assembly

[1] G. M. Whitesides, B. Grzybowski, *Science* **2002**, *295*, 2418.
[2] T. Thurn-Albrecht, J. Schotter, C. A. Kastle, N. Emley, T. Shibauchi, L. Krusin-Elbaum, K. Guarini, B. C. T. , M. T. Tuominen, T. P. Russell, *Science* **2000**, *290*, 2126.
[3] V. V. Tsukruk, H. Ko, S. Peleshanko, *Phys. Rev. Lett.* **2004**, *92*, 065502.
[4] H. Ko, V. V. Tsukruk, *Nano Lett.* **2006**, *6*, 1443.
[5] Y. Lin, A. Boker, J. He, K. Sill, H. Xiang, C. Abetz, X. Li, J. Wang, T. Emrick, S. Long, Q. Wang, A. Balazs, T. P. Russell, *Nature* **2005**, *434*, 55.
[6] M. Gleiche, L. F. Chi, H. Fuchs, *Nature* **2000**, *403*, 173.
[7] J. Huang, F. Kim, A. R. Tao, S. Connor, P. D. Yang, *Nat. Mater.* **2005**, *4*, 896.
[8] A. M. Kalsin, M. Fialkowski, M. Paszewski, S. K. Smoukov, K. J. M. Bishop, B. A. Grzybowski, *Science* **2006**, *312*, 420.
[9] R. D. Deegan, O. Bakajin, T. F. Dupont, G. Huber, S. R. Nagel, T. A. Witten, *Nature* **1997**, *389*, 827.
[10] R. D. Deegan, O. Bakajin, T. F. Dupont, G. Huber, S. R. Nagel, T. A. Witten, *Phys. Rev. E* **2000**, *62*, 756.
[11] E. Rabani, D. R. Reichman, P. L. Geissler, L. E. Brus, *Nature* **2003**, *426*, 271.
[12] T. P. Bigioni, X. M. Lin, T. T. Nguyen, E. I. Corwin, T. A. Witten, H. M. Jaeger, *Nat. Mater.* **2006**, *5*, 265.
[13] V. L. Colvin, M. C. Schlamp, A. P. Alivisatos, *Nature* **1994**, *370*, 354.
[14] W. U. Huynh, J. J. Dittmer, A. P. Alivisatos, *Science* **2002**, *295*, 2425.
[15] I. L. Medintz, H. T. Uyeda, E. R. Goldman, H. Mattoussi, *Nat. Mater.* **2005**, *4*, 435.
[16] J. Xu, J. Xia, J. Wang, J. Shinar, Z. Q. Lin, *Appl. Phys. Lett.* **2006**, *89*, 133110.
[17] S. W. Hong, J. Xu, J. Xia, Z. Q. Lin, F. Qiu, Y. L. Yang, *Chem. Mater.* **2005**, *17*, 6223.
[18] J. Xu, J. Xia, S. W. Hong, Z. Q. Lin, F. Qiu, Y. L. Yang, *Phys. Rev. Lett.* **2006**, *96*, 066104.
[19] S. W. Hong, J. Xu, Z. Q. Lin, *Nano Lett.* **2006**, *6*, 2949.
[20] S. W. Hong, S. Giri, V. S. Y. Lin, Z. Q. Lin, *Chem. Mater.* **2006**, *18*, 5164.
[21] S. W. Hong, J. Xia, Z. Q. Lin, *Adv. Mater.* **2007**, in press.
[22] E. Adachi, A. S. Dimitrov, K. Nagayama, *Langmuir* **1995**, *11*, 1057.
[23] L. Shmuylovich, A. Q. Shen, H. A. Stone, *Langmuir* **2002**, *18*, 3441.
[24] Z. Q. Lin, S. Granick, *J. Am. Chem. Soc.* **2005**, *127*, 2816.
[25] N. D. Denkov, D. Velev, P. A. Kralchevsky, I. B. Ivanov, H. Yoshimura, K. Nagayamat, *Langmuir* **1992**, *8*, 3183.
[26] N. V. Churaev, *Liquid and Vapor Flows in Porous Bodies. Surface Phenomena*, *Vol. 13*, Gordon and Breach, University of Salford, **2000**.
[27] A. V. Lyushnin, A. A. Golovin, L. M. Pismen, *Phys. Rev. E* **2002**, *65*, 021602.
[28] P. J. Pauzauskie, D. J. Sirbuly, P. D. Yang, *Phys. Rev. Lett.* **2006**, *96*, 143903.
[29] A. M. Cazabat, F. Heslot, S. M. Troian, P. Carles, *Nature* **1990**, *346*, 824.
[30] O. Karthaus, L. Grasjo, N. Maruyama, M. Shimomura, *Chaos* **1999**, *9*, 308.
[31] I. Leizerson, S. G. Lipson, A. V. Lyushnin, *Langmuir* **2004**, *20*, 291.
[32] X. Michalet, R. Ekong, F. Fougerousse, S. Rousseaux, C. Schurra, N. Hornigold, M. van Slegtenhorst, J. Wolfe, S. Povey, J. S. Beckmann, A. Bensimon, *Science* **1997**, *277*, 1518.
[33] X. Peng, L. Manna, W. D. Yang, J. Wickham, E. Scher, C. Kadavanich, A. P. Alivisatos, *Nature* **2000**, *404*, 59.
[34] M. Green, P. O'Brian, *Chem. Commun.* **2000**, 183.

